Applied Physics Express

Charge transport and activation energy of amorphous silicon carbide thin film on quartz at elevated temperature

To cite this article: Toan Dinh *et al* 2015 *Appl. Phys. Express* **8** 061303

View the article online for updates and enhancements.

Related content

- Thickness Dependences of Resistivity and Temperature Coefficient of Resistance for Ge Thin Films Sandwiched between Si Layers for Uncooled Infrared Imaging Sensor
Kazuhiro Yamaki, Takashi Tai, Junichi Kinoshita et al.
- Electrical properties of a-SiC/c-Si(p) heterojunctions
L Magafas, N Georgoulas and A Thanailakis
- Fabrication of Vanadium Oxide Thin Films on Fused Quartz Substrates by Metal–Organic Decomposition for Bolometer Detectors
Le Ngoc Son, Takashi Tachiki and Takashi Uchida

Recent citations

- Confinement induced variation of composition ratio in amorphous silicon carbide thin films and effect in optical properties
Aakash Mathur *et al*
- Advances in Rational Design and Materials of High-Performance Stretchable Electromechanical Sensors
Toan Dinh *et al*
- Jarred Fastier-Wooller *et al*

This content was downloaded from IP address 132.234.88.244 on 14/03/2021 at 23:02

Applied Physics Express **8**, 061303 (2015)
http://dx.doi.org/**10.7567/APEX.8.061303**

Charge transport and activation energy of amorphous silicon carbide thin film on quartz at elevated temperature

Toan Dinh[1], Dzung Viet Dao[1,2*], Hoang-Phuong Phan[1], Li Wang[1], Afzaal Qamar[1], Nam-Trung Nguyen[1], Philip Tanner[1], and Maksym Rybachuk[2]

[1]*Queensland Micro- and Nanotechnology Centre, Griffith University, Nathan Qld 4111, Australia*
[2]*School of Engineering, Griffith University, Gold Coast Qld 4222, Australia*
E-mail: d.dao@griffith.edu.au

Received April 2, 2015; accepted April 30, 2015; published online May 26, 2015

We report on the temperature dependence of the charge transport and activation energy of amorphous silicon carbide (a-SiC) thin films grown on quartz by low-pressure chemical vapor deposition. The electrical conductivity as characterized by the Arrhenius rule was found to vary distinctly under two activation energy thresholds of 150 and 205 meV, corresponding to temperature ranges of 300 to 450 K and 450 to 580 K, respectively. The a-SiC/quartz system displayed a high temperature coefficient of resistance ranging from −4,000 to −16,000 ppm/K, demonstrating a strong feasibility of using this material for highly sensitive thermal sensing applications. © 2015 The Japan Society of Applied Physics

The need for sensors and circuits that can operate in hostile environments has motivated recent research on materials with a large energy band gap. Among these materials, silicon carbide (SiC) is one of the most promising candidates owing to its superior physical properties and the availability of its wafers.[1)] Various studies have investigated the sensitivity of SiC to strain/stress for mechanical sensors.[2–7)] Owing to the relatively large temperature coefficient of resistance (TCR), SiC has also been deployed in several thermal sensing devices.[8–11)]

One of the main drawbacks of SiC is the high cost of its wafers compared to conventional silicon (Si). Growing a thin single-crystal functional SiC film on Si substrates or an amorphous SiC (a-SiC) film on glass or quartz substrates would reduce the cost of bulk SiC wafers. For instance, the commercial price of crystalline 4H-SiC or 6H-SiC wafers is approximately one order of magnitude higher than that of a-SiC/Si wafers.[12)] Therefore, recent research has focused on improving the growth process in order to enhance the quality of SiC films and to reduce the cost.[13)] The a-SiC film deposited on quartz by low-pressure chemical vapor deposition (LPCVD) would offer great economic advantages because it could be uniformly deposited on a large-area quartz substrate.

For thermal sensing devices such as temperature sensors,[8–11)] flow sensors,[14)] and inertial sensors,[15,16)] the temperature dependence of the electrical properties needs to be known, as it provides information about the sensitivity and system energies.[17)] Although common amorphous materials such as silicon (a-Si), hydrogenated silicon, and germanium have been investigated,[18–20)] the temperature-dependent electrical properties of a-SiC thin films grown on quartz have not been reported.

In this letter, we report on the temperature dependence of charge transport in an a-SiC film grown on a fused quartz substrate by LPCVD. By analyzing the Arrhenius characteristics of the a-SiC/quartz system, we determine the activation energy in the 300 to 580 K temperature range. We demonstrate a strong feasibility of using a-SiC thin films for sensitive thermal sensing applications.

The SiC film was deposited on a fused quartz substrate (1 in. square, 2 mm thick) using a hot-wall reactor at 650 °C. Monomethylsilane (H_3SiCH_3) was employed as a single precursor at 9.5 sccm, and deposition was performed for 10 h at a pressure of 0.6 Pa.

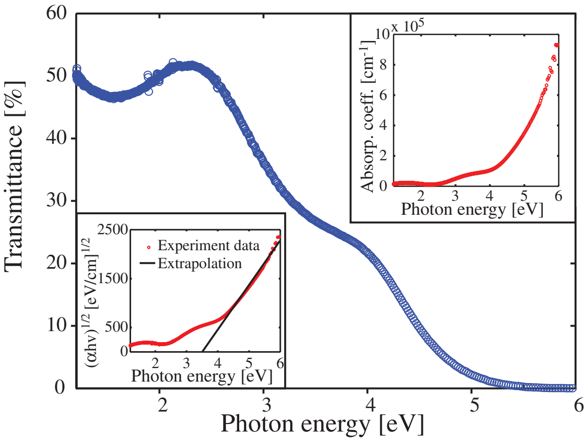

Fig. 1. Transmittance spectra of the a-SiC film. Bottom-left inset shows the derived optical energy gap, and top-right inset presents the derived optical absorption spectra.

As-deposited a-SiC thin films were found to be ~95 ± 3 nm thick with a surface roughness of ~10 ± 3 nm, as determined from spectroscopic ellipsometry measurements (M-2000, J. A. Woolam) in reflection mode using a variable-angle (55–75°) sampling in the 245–1600 nm range. Transmittance values obtained using a PerkinElmer double-beam spectrometer at normal incidence angles in the 200–1100 nm range are shown in Fig. 1. The graph of $(\alpha h\upsilon)^{1/2}$ versus $h\upsilon$ (the bottom-left inset in Fig. 1), where α, h, and υ are the optical absorption coefficient, Planck's constant, and the frequency of the radiation, respectively, indicates that the optical energy gap E_g is 3.5 eV, which is wider than that of single-crystalline 3C-SiC (2.3 eV).[21)] This result agrees with an optical gap value of 3.3 eV obtained using spectroscopic ellipsometry measurements in reflection mode. In addition, the top-right inset in Fig. 1 indicates that the absorption coefficient is on the order of $10^5\,cm^{-1}$, which is approximately two orders of magnitude higher than that of single-crystalline 3C-SiC.[22)] The polarity of the hot probe voltage was used to determine the type of electrical conductivity in a-SiC materials, and the fabricated a-SiC material was found to display n-type conductivity.

Figure 2 shows the experimental setup for characterization of the thermoresistive effect in a-SiC films. A 25 mm × 25 mm strip was placed on top of a hot plate (RT Stirring,

 © 2015 The Japan Society of Applied Physics

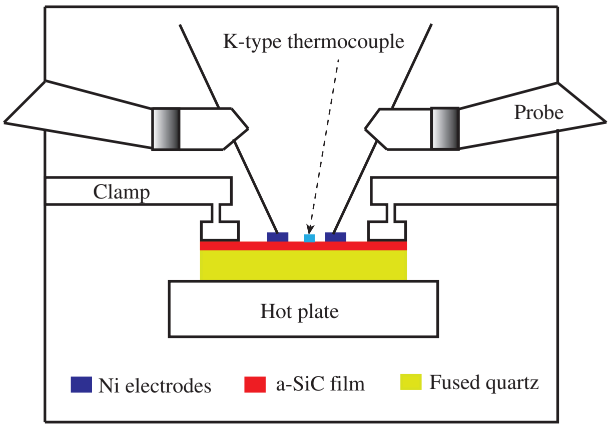

Fig. 2. Schematic sketch of experimental setup (not to scale).

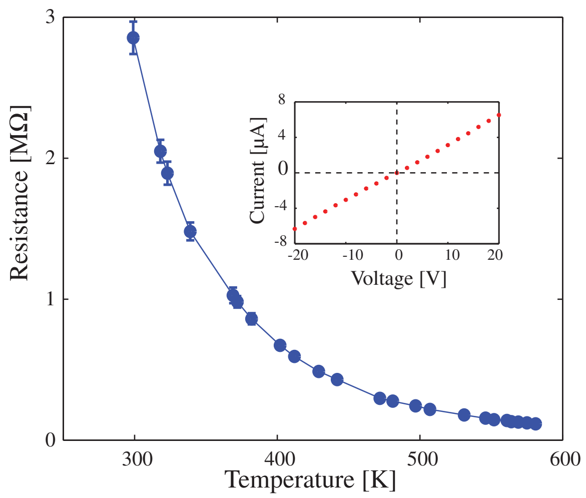

Fig. 3. Thermoresistive characteristics of a-SiC films (inset shows the *I–V* curve).

Thermo Scientific) and was fixed by two clamps. The surface temperature of the strip was determined by a K-type thermocouple (resolution 1 °C, accuracy ±3%). Probe tips were pushed against the sputter-deposited nickel electrodes to electrically connect the films. The resistance of the a-SiC films was monitored by an ohmmeter (Fluke 117) with a resolution of 0.1 Ω.

The inset of Fig. 3 shows good ohmic contact between the sputtered Ni contacts and the a-SiC, whereas Fig. 3 shows the electrical resistance versus temperature for the a-SiC thin film. The significant decrease in the resistance with increasing temperature indicates that the conduction of a-SiC is thermally activated. When the temperature is increased from 300 to 580 K, the resistance of a-SiC is observed to decrease by two orders of magnitude from the megohm to the kilo-ohm range; this phenomenon can be explained as follows.

Generally, the conductivity σ of a-SiC can be calculated as

$$\sigma = e\int \mu(\epsilon)n(\epsilon)\,d\epsilon, \tag{1}$$

where e is the electron charge, and $\mu(\epsilon)$ and $n(\epsilon)$ are the electron mobility and the electron concentration in the states at energy level ϵ, respectively. If the temperature is high enough,[23] the conductivity is dominated by the states with an energy range k_BT above the mobility edge ϵ_c (where k_B is the Boltzmann constant). Then σ can be approximately estimated as

$$\sigma = e\mu_c g(\epsilon_c)f(\epsilon_c)k_BT, \tag{2}$$

where μ_c is the electron mobility above ϵ_c, $g(\epsilon_c)$ is the density of states (DOS), and $f(\epsilon_c) = 1/[1 + \exp((\epsilon_c - \epsilon_F)/k_BT)]$ is the Fermi function depending on the Fermi energy ϵ_F. Therefore, the conductivity σ of a-SiC can be expressed in the form[23]

$$\sigma = \sigma_0 \exp\left[-\left(\frac{E_a}{k_BT}\right)^{\beta}\right], \tag{3}$$

where σ_0 is the pre-exponential factor, and the exponent β depends on the temperature range. E_a denotes the activation energy. There have been various models that define the conductivity regimes of amorphous materials well. It is believed that at low temperatures (e.g., $T < 300$ K), the temperature-dependent conductivity of a-SiC follows the variable-range hopping (VRH) theory of Mott and Davis,[24] in which the transport energy is situated deep in the band tail, and transitions between localized states below the mobility edge are considered to be dominant. The tunneling conduction of an electron moving from one localized state to another localized state depends on the spatial separation and energy levels of the states. If the DOS is constant, the value of β in Eq. (3) was found to be 1/4 for the VRH regime. However, if the DOS follows a parabolic function, the obtained value of $\beta = 1/2$ indicates the presence of the Coulomb pseudogap.[23]

Fitting the experimental data for a-SiC in the temperature range from 300 to 580 K using the model described by Eq. (3) revealed the following. The best lineshape was found for the value of $\beta = 1$ and the constant pre-exponent factor, σ_0, at which conduction in the fabricated a-SiC follows the well-known Arrhenius law. This result indicates that electrons are activated over the mobility edge when they move between the delocalized states above the mobility edge and the localized tail band.[25,26] The extended states remain delocalized as a result of energy perturbations. As the increase in the temperature causes thermally activated phonons to induce delocalization of states, the electrical conductivity of an a-SiC material is expected to increase.

The temperature-dependent resistance R can be described using the following form:

$$R \propto \exp\left(-\frac{E_a}{k_BT}\right), \tag{4}$$

where $E_a = \epsilon_c - \epsilon_F$. Therefore, the relationship between the change in the conductivity and the temperature (shown in Fig. 4) is defined as

$$-\ln(\sigma/\sigma_0) = E_a(k_BT)^{-1} - b, \tag{5}$$

where $b = E_a(k_BT_0)^{-1}$ is a constant (T_0 is the reference temperature). From the slope of the fitted lineshape, the activation energy, E_a, was found to be 150 meV in the temperature range from 300 to 450 K and to increase to 205 meV at higher temperatures such as 450 to 580 K. The obtained results are comparable to those attributed to an a-Si material reported by Abtew et al.,[19] which exhibited E_a values of 340 meV at temperatures below 450 K and 450 meV at temperatures above 450 K. The calculated ratio of $2E_a/E_g$ was found to be

© 2015 The Japan Society of Applied Physics

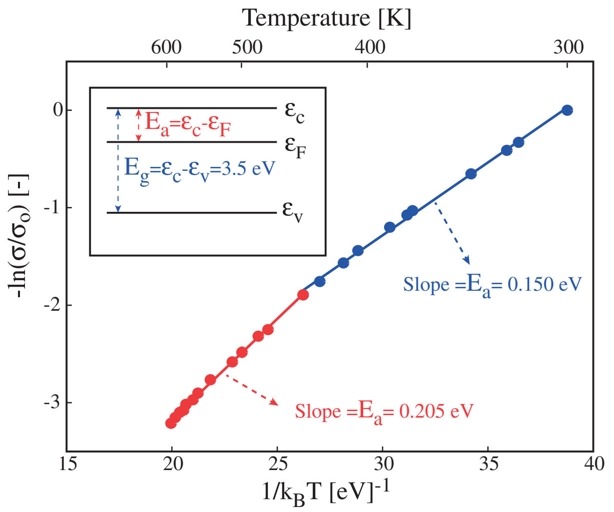

Fig. 4. Arrhenius plot of a-SiC thermoresistance. Inset shows sketch of energy levels in n-type a-SiC (not to scale).

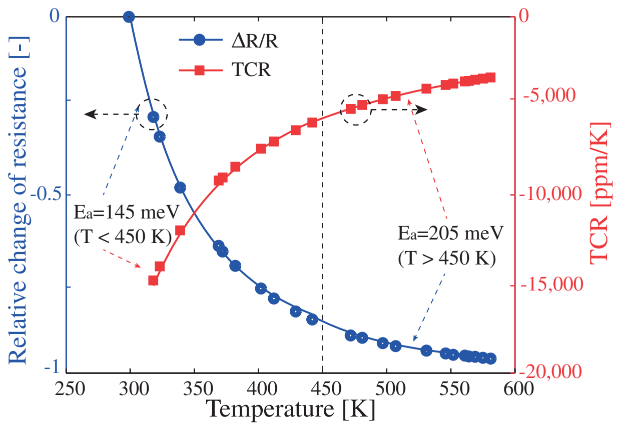

Fig. 5. Relative change in resistance $\Delta R/R$ and TCR of a-SiC films.

less than unity, indicating that the Fermi energy level is located in the upper region of the forbidden band (inset in Fig. 4).[27] This result also confirms that the fabricated a-SiC material is of an n-type, as initially determined by the hot probe measurements.

A significant feature of the fabricated a-SiC material is its high TCR. The TCR is expressed in the following form:

$$\mathrm{TCR} = \frac{\Delta R}{R}\frac{1}{\Delta T} = \frac{\exp\left[E_a\left(\dfrac{1}{k_BT} - \dfrac{1}{k_BT_0}\right)\right] - 1}{T - T_0}, \qquad (6)$$

where $\Delta R/R$ is the relative change in the resistance of a-SiC, and $\Delta T = T - T_0$ is the temperature difference. The $\Delta R/R$ and TCR functions are fitted well by Eq. (6) and the defined E_a values, as shown in Fig. 5. The obtained $\Delta R/R$ ratio is found to be approximately 96% at 580 K. The absolute TCR value is larger than 4000 ppm/K for temperatures from 300 to 580 K. The TCR value is found to be significantly higher than that of a-SiC materials fabricated by a sputtering process, as reported by Fraga et al.[28] (~40 ppm/K); therefore, it shows an enhanced technological potential for thermal sensing applications. The high TCR of the a-SiC film grown by LPCVD is attributed to the fact that the LPCVD process

Table I. List of thermistor coefficients in this work and the literature.

Material	Technique	Temp. (K)	B coeff. (K)
a-SiC*	LPCVD	300–580	1750–2400
SiC/Diamond/Si[9]	MPCVD	300–570	550–4500
3C-SiC[10]	Rf-sputtering	200–720	1600–3400
3C-SiC[11]	Rf-sputtering	275–770	2000–4000
3C-SiC[8]	CVD	300–670	5000–7000

*Indicates the result in this study.

typically produces high-quality a-SiC films with better purity, uniformity, and lattice homogeneity and fewer defects than a-SiC films fabricated by sputtering processes. In addition, resistors made of a-SiC materials display high sensitivity near room temperature, for example, an absolute TCR value of ~16,000 ppm/K at 25 °C.

As the electrical resistance of an a-SiC material is governed by Eq. (4), the resistance versus temperature characteristics of an a-SiC material can be described by the thermistor equation, $R = R_0 \exp[B(1/T - 1/T_0)]$, where B is the thermistor coefficient and can be calculated as $B = E_a/k_B$. The B value is higher at higher temperatures, indicating domination of the donor states; for example, it is approximately 2400 and 1750, corresponding to E_a values of 205 and 150 meV, respectively. The obtained thermistor coefficient values are comparable to those for other SiC-based thermistor materials, as shown in Table I. The obtained result confirms that the fabricated a-SiC thin-film material on quartz forms a sensitive temperature-sensing element.

In summary, the charge transport and activation energy of an a-SiC thin-film material grown on fused quartz by LPCVD were investigated, and the electrical conduction mechanism of the a-SiC material was studied. The thermal activation energies for the fabricated a-SiC were found to be 150 and 205 meV for temperature ranges of 300 to 450 K and 450 to 580 K, respectively. The fabricated a-SiC/quartz system displayed large negative values of the temperature coefficient of resistance, demonstrating a strong feasibility of using this material for highly sensitive thermal sensing applications.

Acknowledgment This work was performed in part at the Queensland node of the Australian National Fabrication Facility, a company established under the National Collaborative Research Infrastructure Strategy to provide nano- and microfabrication facilities for Australia's researchers; MR acknowledges the Sir Samuel Griffith Program for research support.

1) V. Cimalla, J. Pezoldt, and O. Ambacher, J. Phys. D **40**, 6386 (2007).
2) C.-H. Wu, C. A. Zorman, and M. Mehregany, IEEE Sens. J. **6**, 316 (2006).
3) H. P. Phan, P. Tanner, D. V. Dao, N. T. Nguyen, L. Wang, Y. Zhu, and S. Dimitrijev, IEEE Electron Device Lett. **35**, 399 (2014).
4) H. P. Phan, D. V. Dao, P. Tanner, N. T. Nguyen, L. Wang, Y. Zhu, and S. Dimitrijev, Appl. Phys. Lett. **104**, 111905 (2014).
5) H. P. Phan, D. V. Dao, P. Tanner, N. T. Nguyen, J. S. Han, S. Dimitrijev, G. Walker, L. Wang, and Y. Zhu, J. Mater. Chem. C **2**, 7176 (2014).
6) A. Qamar, P. Tanner, D. V. Dao, H. P. Phan, and T. Dinh, IEEE Electron Device Lett. **35**, 1293 (2014).
7) H. P. Phan, D. V. Dao, L. Wang, T. Dinh, N. T. Nguyen, A. Qamar, P. Tanner, S. Dimitrijev, and Y. Zhu, J. Mater. Chem. C **3**, 1172 (2015).
8) E. A. de Vasconcelos, S. A. Khan, W. Y. Zhang, H. Uchida, and T. Katsube, Sens. Actuators A **83**, 167 (2000).
9) S. Yonekubo, K. Kamimura, and Y. Onuma, Proc. Transducers '95, 1995, p. 116.

© 2015 The Japan Society of Applied Physics

10) K. Wasa, T. Tohda, Y. Kasahara, and S. Hayakawa, Rev. Sci. Instrum. **50**, 1084 (1979).
11) T. Nagai and M. Itoh, IEEE Trans. Ind. Appl. **26**, 1139 (1990).
12) Web [http://www.mtixtl.com/search.aspx?find=%2csic+wafer].
13) L. Wang, A. Iacopi, S. Dimitrijev, G. Walker, A. Fernandes, L. Hold, and J. Chai, Thin Solid Films **564**, 39 (2014).
14) N.-T. Nguyen, IEEE Sens. J. **5**, 1224 (2005).
15) D. V. Dao, V. T. Dau, T. Shiozawa, and S. Sugiyama, J. Microelectromech. Syst. **16**, 950 (2007).
16) V. T. Dau, D. V. Dao, and S. Sugiyama, Smart Mater. Struct. **16**, 2308 (2007).
17) O. Chauvet, Phys. Rev. B **46**, 8139 (1992).
18) M. A. Kastner, G. S. Thomas, and S. R. Ovshinsky, *Disordered Semiconductors* (New York, 1987) p. 499.
19) T. A. Abtew, M. Zhang, and D. A. Drabold, Phys. Rev. B **76**, 045212 (2007).
20) C. Bapanayya, R. Gupta, and S. C. Agarwal, Philos. Mag. Lett. **91**, 134 (2011).
21) R. G. Humphreys, D. Bimberg, and W. J. Choyke, Solid State Commun. **39**, 163 (1981).
22) L. Patrick and W. J. Choyke, Phys. Rev. **186**, 775 (1969).
23) S. Baranovski, *Charge Transport in Disordered Solids with Applications in Electronics* (John Wiley and Sons, 2006) p. 50.
24) N. F. Mott and E. A. Davis, *Electronic Processes in Non-Crystalline Materials* (Oxford, 1979) 2nd ed., p. 32.
25) R. A. Street, *Hydrogenated Amorphous Silicon* (Cambridge, 1991) p. 227.
26) P. Fenz, H. Muller, H. Overhof, and P. Thomas, J. Phys. C **18**, 3191 (1985).
27) S. Hariech, M. S. Aida, and H. Moualkia, Mater. Sci. Semicond. Process. **15**, 181 (2012).
28) M. A. Fraga, H. Furlan, L. A. Rasia, and L. L. Koberstein, ECS Trans. **44** [1], 1375 (2012).

© 2015 The Japan Society of Applied Physics